Critical Roles of the Stratiform Rainfall in Sustaining the Madden–Julian Oscillation: GCM Experiments*

XIOUHUA FU

IPRC, SOEST, University of Hawaii at Manoa, Honolulu, Hawaii

BIN WANG

IPRC, SOEST, and Department of Meteorology, University of Hawaii at Manoa, Honolulu, Hawaii

(Manuscript received 30 April 2008, in final form 6 February 2009)

ABSTRACT

This study assesses the impact of stratiform rainfall (i.e., large-scale rainfall) in the development and maintenance of the Madden–Julian oscillation (MJO) in a contemporary general circulation model: ECHAM4 AGCM and its coupled version. To examine how the model MJO would change as the stratiform proportion (the ratio of the stratiform versus total rainfall) varies, a suite of sensitivity experiments has been carried out under a weather forecast setting and with three 20-yr free integrations. In these experiments, the detrainment rates of deep/shallow convections that function as a water supply to stratiform clouds were modified, which results in significant changes of stratiform rainfall.

Both the forecast experiments and long-term free integrations indicate that only when the model produces a significant proportion ($\geq$30%) of stratiform rainfall can a robust MJO be sustained. When the stratiform rainfall proportion becomes small, the tropical rainfall in the model is dominated by drizzle-like regimes with neither eastward-propagating nor northward-propagating MJO being sustained.

It is found that the latent heat release of stratiform rainfall significantly warms up the upper troposphere. The covariability between the heating and positive temperature anomaly produces eddy available potential energy that sustains the MJO against dissipation and also allows the direct interaction between the precipitation heating and large-scale low-frequency circulations, which is critical to the development and maintenance of the MJO. This finding calls for better representations of stratiform rainfall and its connections with the convective component in GCMs in order to improve their simulations of the MJO.

1. Introduction

The active and break phases of the Madden–Julian oscillation (MJO) strongly modulate the development of severe synoptic weather systems: For example, hurricanes (Maloney and Hartmann 2000; Bessafi and Wheeler 2006) and monsoon depressions (Chen and Weng 1999; Goswami et al. 2003). The recurrent nature of MJO with a period of 30–60 days (Madden and Julian 1972; Yasunari 1979) offers an opportunity to forecast the active/break phase of this low-frequency wave with a lead time up to a month or longer (Fu et al. 2007; Miura et al. 2007; Fu et al. 2008a; Bechtold et al. 2008). Knowing the approach of extreme MJO phases warrants a forecast of weather statistics beyond the conventional deterministic synoptic forecast (~one week). This capability fills the gap between medium-range weather forecast and seasonal climate outlook (Waliser 2005), contributing to the realization of seamless forecast, which is one of the overarching goals of the World Climate Research Programme (WCRP) (Toth et al. 2007; Moncrieff et al. 2007).

Unfortunately, many contemporary general circulation models (GCMs) still have tremendous difficulties to realistically simulate MJO (Waliser et al. 2003a; Lin et al. 2006; H.-M. Kim et al. 2008; Sperber and Annamalai

* School of Ocean and Earth Science and Technology Contribution Number 7670 and International Pacific Research Center Contribution Number 602.

Corresponding author address: Dr. Joshua Xiouhua Fu, International Pacific Research Center, SOEST, University of Hawaii at Manoa, 1680 East-West Road, POST Bldg. 409D, Honolulu, HI 96822.
E-mail: xfu@hawaii.edu

DOI: 10.1175/2009JCLI2610.1

2008). Though the exact reasons for model caveats are still unknown, many believe that the primary modeling problems lie in the inadequate representations of moist convection (Tokioka et al. 1988; Wang and Schlesinger 1999; Maloney and Hartmann 2001; and others) and the multiscale interaction processes (Wang 2005) as well as the lack of efficient air–sea coupling (Waliser et al. 1999; Hendon 2000; Fu et al. 2003; Fu and Wang 2004).

The sensitivity of MJO simulations to various cumulus parameterization schemes has been evaluated extensively but the conclusions are controversial. Based on comparing the MJO simulated in 15 GCMs, Slingo et al. (1996) found that the quality of the simulated MJO is strongly linked to the type of closure used in the convective parameterization, with buoyancy closure being preferable to moisture convergence. On the other hand, Lin et al. (2006), based on comparing the MJO simulated in 14 GCMs participating in Intergovernmental Panel on Climate Change (IPCC) Fourth Assessment Report (AR4), suggested the opposite: models with moisture-convergence closure produce better MJO than those closed with buoyancy. Liu et al. (2005) replaced the Zhang and McFarlane convective scheme with the Tiedtke scheme in the National Center for Atmospheric Research (NCAR) Community Atmosphere Model, version 2 (CAM2) and found that the model MJO was significantly improved. Chao and Deng (1998) and Lee et al. (2003) compared three different schemes, the moist convective adjustment (MCA), Kuo scheme, and the modified Arakawa–Schubert (AS) scheme (Arakawa and Schubert 1974). Both studies found that MCA produces the strongest MJO while the AS scheme produces the weakest. Tokioka et al. (1988) significantly improved the MJO simulation in their GCM by introducing a nonzero minimum cumulus entrainment rate (functioning like a delayed mechanism for the onset of deep convection) into the AS scheme. Wang and Schlesinger (1999) found that a large relative humidity threshold in convective parameterization is critical for the amplification of the MJO by causing a time lag between condensational heating and large-scale convergence. Yet, Maloney and Hartmann's (2001) sensitivity experiments with the Community Climate Model, version 3.6 (CCM3.6) indicated that the model MJO is not sensitive to the relative humidity threshold.

These diversified and sometime controversial findings on the ways to improve the simulation of MJO pose a great challenge to transfer an individual model's success to the others. The lack of consensus on this issue most likely originates from the lack of enough reliable observations to validate the model MJO, particularly the three-dimensional spatial–temporal evolutions of MJO. Even ''good'' model simulations may be attributed to the wrong physical reasons (e.g., error cancellations). An outstanding open question is the following: What are the critical pieces of model physics for the realistic simulation of MJO that have been missed or misrepresented in many contemporary GCMs?

The stratiform clouds associated with convective plumes may be a misrepresented process in many contemporary general circulation models (Lin et al. 2004). Using Tropical Rainfall Measuring Mission (TRMM) precipitation radar (PR) data, Schumacher and Houze (2003) found that stratiform precipitation accounts for more than 40% of the total rain amount in the global tropics (20°S–20°N). Wang et al. (2006), also using the TRMM PR data, revealed that the boreal summer MJO convection comprises a significant stratiform component, particularly during its initiation and developing stages in the equatorial Indian Ocean. Some theoretical studies (Cho and Pendlebury 1997; Mapes 2000; Straub and Kiladis 2003; Khouider and Majda 2006; Kuang 2008) have emphasized the stratiform clouds as an important process to maintain the low-frequency instability associated with equatorial convectively coupled waves. In nature, stratiform rainfall is evolved from and intimately related to convective clouds (Leary and Houze 1980; Houze 1997). In the ECHAM4 model, the stratiform rainfall (i.e., large-scale rainfall) is parameterized as a function of environmental humidity (Sundqvist 1978) and is connected to convective clouds largely through the entrainments and detrainments of cumulus ensembles (Tiedtke 1989).

The ECHAM family models have been recognized as one of the best contemporary global models with reasonably realistic simulations of MJO in both winter and summer (Sperber et al. 2005; Lin et al. 2006; H.-M. Kim et al. 2008; Sperber and Annamalai 2008). In this study, a series of sensitivity experiments have been conducted with the ECHAM4 AGCM and its coupled version, intending to unravel the important physical processes that maintain the MJO in this model. Special attention has been given to the sensitivity of model MJO to the fraction of stratiform rainfall and environmental humidity (Derbyshire et al. 2004).

In section 2, the ECHAM4 coupled model is briefly introduced along with an introduction of the details of all sensitivity experiments. Section 3 validates the model MJO with the tools developed by the U.S. Climate Variability and Predictability (CLIVAR) MJO working group (http://www.usclivar.org/Organization/MJO_WG.html). Section 4 examines the sensitivity of model MJO to the fraction of stratiform rainfall under a weather forecast setting and the impact of stratiform rainfall on the long-term simulation of MJO with three 20-yr free integrations. The physical processes that may be relevant

to explain the GCM results are discussed in section 5. The last section summarizes our major findings.

2. Model and experimental designs

a. ECHAM4 coupled model

ECHAM4 AGCM was developed by the Max Plank Institute for Meteorology in Germany (Roeckner et al. 1996). The version we used in this study has a horizontal resolution of about 3.75° in both longitude and latitude (T30), with 19 vertical levels extending from the surface to 10 hPa. The mass flux scheme of Tiedtke (1989) with a CAPE closure (Nordeng 1995) has been used to parameterize the deep, shallow, and midlevel convections. The ocean component coupled to the ECHAM is a 2½-layer tropical upper-ocean model with a horizontal resolution of 0.5° in both longitude and latitude. It was originally developed by Wang et al. (1995) and improved by Fu and Wang (2001), which combines the mixed layer thermodynamics of Gaspar (1988) and the upper-ocean dynamics of McCreary and Yu (1992). The entrained water temperature is parameterized as a function of thermocline depth, similar to the one used in Jin (1996).

The AGCM and the ocean model are coupled in the tropical Indo-Pacific Oceans (30°S–30°N) without explicit heat flux correction. Outside the coupled region, the underlying SST is specified as the climatological monthly mean SST averaged from 16 yr (1979–94) boundary conditions of Atmospheric Model Intercomparison Project II (AMIP-II) experiments. The atmospheric component exchanges information with the ocean component once per day. The initial atmospheric and ocean conditions are from the restart files of a long-term coupled integration.

This coupled model simulates monsoon climatology in the Asian–western Pacific region much better than the stand-alone ECHAM4 AGCM does (Fu et al. 2002). It also produces a robust MJO that mimics the one existing in the observations (Kemball-Cook et al. 2002; Fu et al. 2003; Fu and Wang 2004) with coherent spatiotemporal evolutions of rainfall, surface winds, and SST, and reasonable intensity and period (or propagating speed). Using this coupled model, Fu et al. (2007, 2008b) found that interactive air–sea coupling can extend the MJO predictability by about 10 days.

b. Experimental designs

In the ECHAM4 AGCM, stratiform rainfall is represented as grid-scale precipitation (Sundqvist 1978; Sundqvist et al. 1989). A simple cloud microphysics scheme including coalescence of cloud droplets, sedimentation of ice crystals, and the evaporation of precipitation in unsaturated air has been implemented on the model grid scale. The connection between cumulus convection and stratiform clouds in the model is primarily through entrainments and detrainments of cumulus ensembles. The detrained water vapor increases the grid-scale humidity and favors the development of stratiform rainfall. The detrained cloud water from the cumulus ensembles directly serves as a source of stratiform clouds (Roeckner et al. 1996). Both processes mimic the water supply from cumulus updrafts to stratiform anvils as observed in nature (Leary and Houze 1980). In the following sensitivity experiments, we will perturb the convective entrainments and detrainments, thus changing the amount of stratiform rainfall, to see how the model MJO will be influenced.

TABLE 1. Sensitivity experiments under a weather forecast setting.

Expt Name	Description
Fcst01	Coupled control forecast
Fcst02	Set deep-convection entrainment/detrainment rate to zero but keep other parameters as default
Fcst03	Set shallow-convection entrainment/detrainment rate to zero but keep other parameters as default
Fcst04	Keep entrainment/detrainment rates of deep and shallow convection as default; all other entrainment/detrainment rates are set to zero

Two suites of sensitivity experiments have been conducted. One suite is carried out under a weather forecast setting (Phillips et al. 2004). The experiments under a weather forecast setting have been proven to be an efficient way to explore model sensitivity with very short integrations (Xie et al. 2004; Boyle et al. 2005). In total, four experiments have been done under this setting. Details of the experimental designs are given in Table 1. In this case, the ECHAM4 coupled model was initialized with National Centers for Environmental Prediction (NCEP) reanalysis on 1 January 1993 and was integrated for two months. One hundred ensembles have been carried out for each experiment. The initial conditions are perturbed by adding day-to-day root-mean-square differences of four prognostic variables (u, v, T, q) onto the initial NCEP reanalysis fields (Waliser et al. 2003b; Fu et al. 2007). All forecasts target the MJO event observed during the Tropical Ocean and Global Atmosphere Coupled Ocean–Atmosphere Response Experiment (TOGA COARE) in early 1993 (Chen and Yanai 2000). To further corroborate the findings from the forecast experiments, three additional long-term free integrations (20 yr) were also carried out (Table 2).

3. MJO simulated by the ECHAM4 coupled model

In the literature, various atmospheric variables and different methods have been used to measure the model MJO (Slingo et al. 1996; Lin et al. 2006; Zhang et al.

TABLE 2. Sensitivity experiments with long-term free integration.

Expt Name	Description
EX01	Set deep-convection entrainment/detrainment rate to zero and keep other parameters as default
EX02	Set shallow-convection entrainment/detrainment rate to zero and keep other parameters as default
EX03	Both shallow- and deep-convection entrainment/detrainment are allowed

2006). Some of them have been cautioned by Sperber and Annamalai (2008). To put all models under the same screen, the U.S. CLIVAR MJO working group developed reference metrics to measure the MJO simulated by global models (Waliser et al. 2009). The main idea is to quantify the gross feature of MJO: the coupling between diabatic heating [outgoing longwave radiation (OLR) or rainfall] and first baroclinic large-scale circulations (zonal winds at 850 and 200 hPa) as depicted in the seminal paper of Madden and Julian (1972). The details of the metrics and FORTRAN codes can be found in this Web site: http://climate.snu.ac.kr/mjo_diagnostics/index.htm. In this section, several facets of MJO simulated by our ECHAM4 coupled model that have not been extensively documented in previous studies are examined with the metrics provided by this working group. The model output is from a 25-yr free integration of the ECHAM4 coupled model. The observations used to validate the simulations include the Climate Prediction Center (CPC) Merged Analysis of Precipitation (CMAP) rainfall, National Oceanic and Atmospheric Administration (NOAA) OLR, and NCEP reanalysis zonal winds at 850 and 200 hPa. All data span 25 yr from 1980 to 2004.

Figure 1 summarizes the annual-mean standard deviations of 20–100-day filtered rainfall, OLR, and circulation variability from the observations and the simulations. The rainfall and OLR show strongest intraseasonal variance over the Indo–western Pacific warm pool in the tropics (Figs. 1a–d). On the other hand, circulation intraseasonal variability has the largest amplitude in the midlatitude (Figs. 1e–h). The tropical heating perturbations associated with the MJO have been shown to contribute significantly to the midlatitude circulation variability through Rossby wave trains (Liebmann and Hartmann 1984; Weickmann et al. 1985; Hsu 1996; Jones 2000; Ding and Wang 2007). The midlatitude responses may also be amplified by the feedback from synoptic eddies, particularly over the northern Pacific and Atlantic jet regions (Jin et al. 2006; Pan and Li 2008). The ECHAM4 coupled model reproduces almost all intraseasonal action centers in the tropical convection and midlatitude circulations, although the variability of the tropical rainfall and OLR has been modestly exaggerated. Along the equator, the lagged correlations of the 20–100-day filtered OLR have been calculated with a reference point in the eastern Indian Ocean. The result (Fig. 2) shows that the model (Fig. 2b) well captures the coherent eastward propagation of the observed MJO in the Indo–western Pacific Oceans with a slightly faster speed (Fig. 2a).

To compare the life cycles of the observed and model MJO, first two complex empirical orthogonal functions (CEOFs) and their principal components [real-time multivariate MJO series (RMM1, RMM2)] have been extracted from 25-yr observed (1980–2004) and model OLR and zonal winds at 850 and 200 hPa. In addition to the preprocessing of the inputs as used by Wheeler and Hendon (2004), a five-day running mean has also been applied to remove synoptic disturbances (Yang et al. 2008). The resultant two leading CEOFs from the observations and model are very similar to that derived by Wheeler and Hendon (2004). The peak lag correlation between first two principal components for both the model and observations is about 0.7 with a 10-day lag (figures not shown). Based on the derived (RMM1, RMM2) phase-space diagrams, the MJO life cycles have been divided into eight phases. The unfiltered OLR anomalies falling into individual phases have been composited to form the life cycles. Figure 3 compares the boreal winter MJO evolutions for the observations and the simulations. The observed MJO-related convection initiates in the western Indian Ocean and slowly propagates eastward. Both features are well simulated by the ECHAM4 coupled model. The simulation, however, shows a ''double ITCZ'' tendency in the western Pacific (e.g., at phase 3 of Fig. 3). The amplitude of the simulated OLR perturbations is also larger than that in the observations. In boreal summer (Fig. 4), the observed convection primarily propagates northeastward from the equatorial Indian Ocean to the tropical western North Pacific. The model reproduces the major observed propagating feature with comparable amplitude of the OLR perturbations. This brief validation confirms that the ECHAM4 coupled model, in contrast to many other contemporary global models, produces a robust MJO similar to that in the observations.

A question emerges: What are the critical physical processes that sustain the MJO in the ECHAM4 model? As discussed in section 1, the fraction of stratiform rainfall may be one of them. To examine this hypothesis, two suites of sensitivity experiments have been carried out in the following section.

4. Sensitivity of model MJO to the stratiform rainfall

a. Under a weather forecast setting

Figure 5 presents the forecast MJO represented by rainfall and vertical shear of zonal winds between 850

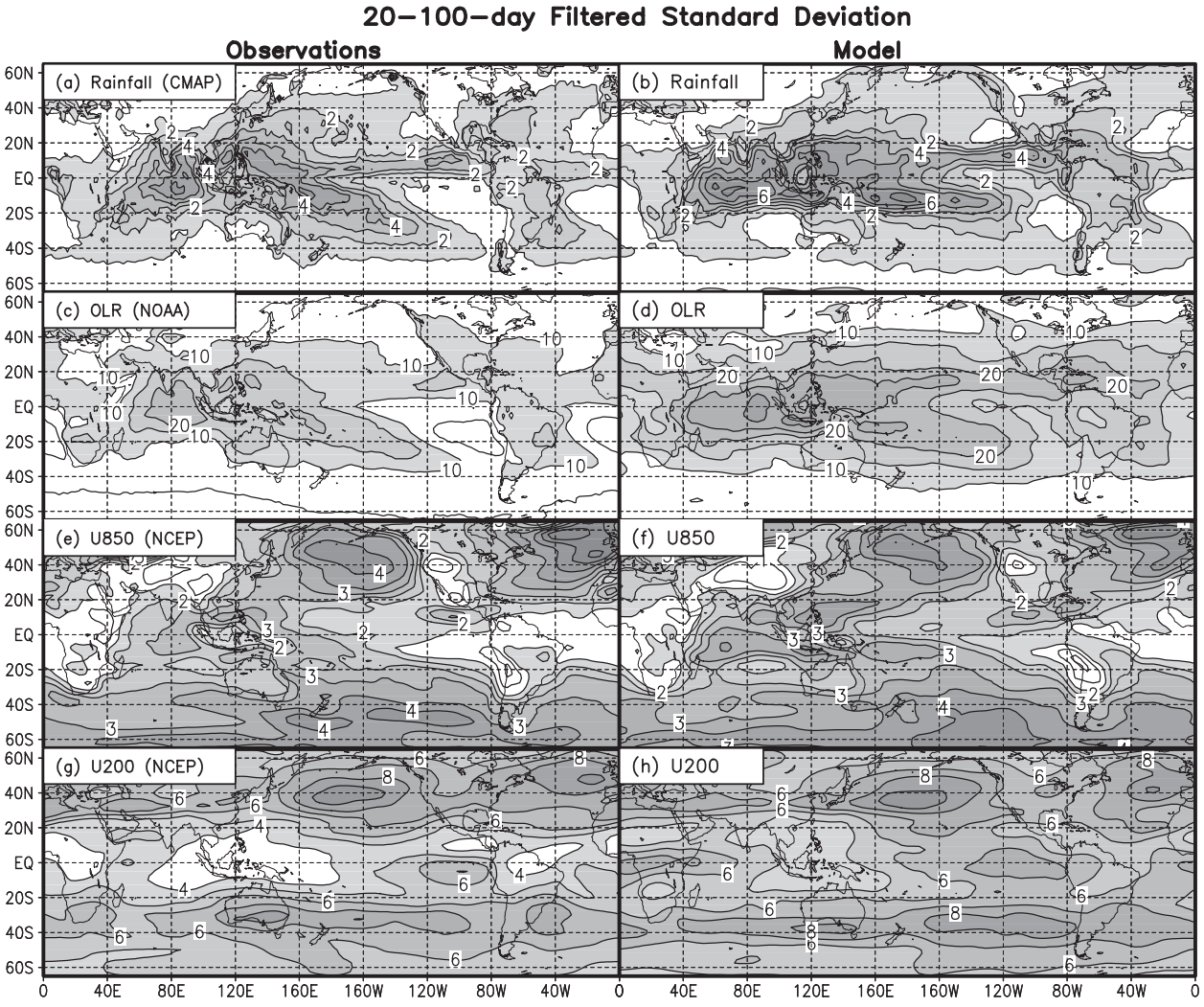

FIG. 1. The (left) observed and (right) simulated spatial distributions of intraseasonal (20–100 day) standard deviations of (a),(b) rainfall (mm day^{-1}); (c),(d) OLR (W m^{-2}); and zonal winds (m s^{-1}) at (e),(f) 850 and (g),(h) 200 hPa.

and 200 hPa in four different experiments. In the control forecast (Fcst01 in Table 1), the coupled model captures the observed quasi-stationary precipitation near the date line (Figs. 5a,b). Then, MJO-related convection is initiated in the western Indian Ocean. The forecast MJO precipitation and associated vertical shear slowly move eastward with a good agreement with the observations even beyond one month.[1] The magnitude of the forecast precipitation averaged from 100 ensembles is smaller than that in the observations.

When no turbulent entrainment/detrainment of deep convection is allowed (Fcst02 in Table 1), the convective plumes reduce their mass and water exchanges with environmental air. The forecast MJO decays quickly after being initiated in the western Indian Ocean (Figs. 5c,d). No apparent eastward propagations of organized convection and associated circulations can be sustained. A similar problem (Figs. 5e,f) appears when the turbulent entrainment/detrainment of shallow convection is turned off (Fcst03 in Table 1). In this case, even the initiation of the MJO-related convection in the western Indian Ocean is jeopardized (Figs. 5e,f).

The above results indicate that the initiation and maintenance of MJO in the ECHAM4 model is sensitive to the turbulent entrainments/detrainments of the deep and shallow convections. In the Tiedtke (1989) mass flux scheme, in addition to the entrainments/detrainments associated with deep and shallow convections, there are other forms of entrainment/detrainment

[1] A cautionary note: The successful simulation of this one MJO event does not indicate that the model has a good MJO forecast skill, which needs to be demonstrated with many more retrospective forecasts.

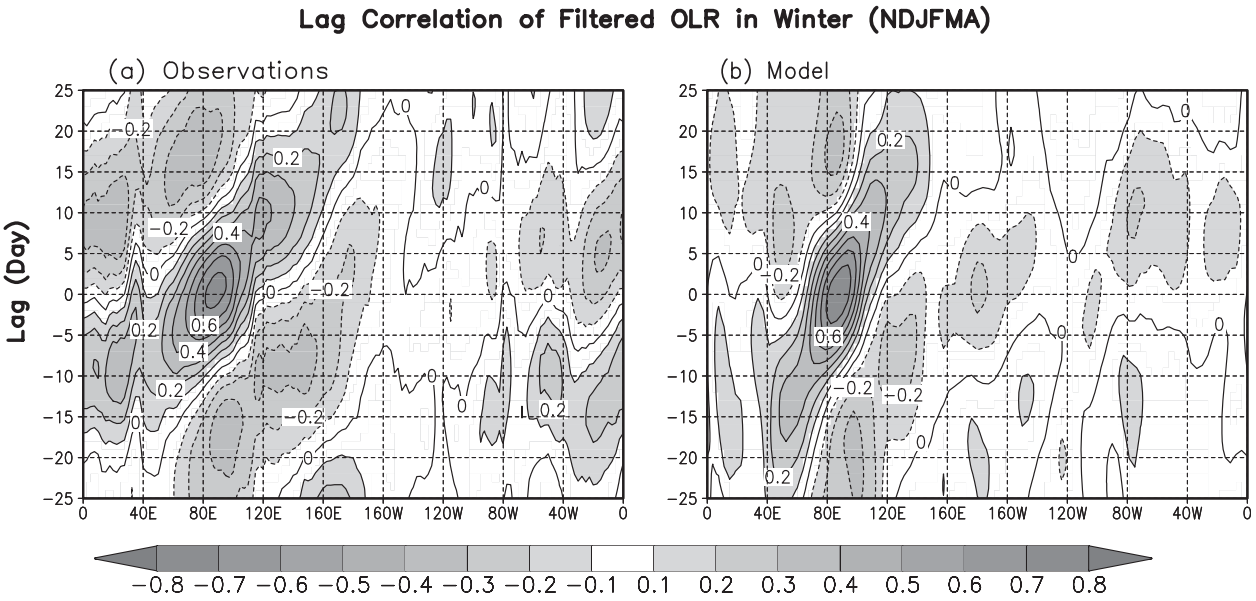

FIG. 2. The lag correlations of 20–100-day filtered OLR along the equator for the (a) observations and (b) simulation.

related to midlevel convection and cumulus downdrafts. In the control forecast (Fcst01 in Table 1), all entrainments/detrainments are activated. To confirm the particular importance of the entrainments/detrainments of deep and shallow convections, one more experiment has been conducted (Fcst04, Table 1) in which all the entrainments/detrainments associated with midlevel convection and cumulus downdrafts are turned off. Figures 5g,h show that the resultant MJO remains in a good agreement with the observations and is very similar to that in the control forecast (Figs. 5a,b).

In addition to the time–longitude plots, another convenient way to view the evolutions of MJO is the phase-space diagram (Wheeler and Hendon 2004). The observed and forecast anomalies of OLR and zonal winds after removing two-month means (from 1 January to 28 February 1993) have been projected onto the two leading CEOFs of the observations, which were derived before. Then, pairs of principle components (RMM1, RMM2) for the observations and forecasts are obtained.

The resultant one-month trajectories of the observations and four experiments are given in Fig. 6. The distances between the initial observation and forecast conditions indicate that further improvement of initialization is needed. The MJOs in four experiments can be divided into two groups: one group (Fcst02 and Fcst03 in Table 1) decays quickly before reaching the Indian Ocean; the events in the other group (Fcst01 and Fcst04 in Table 1) gradually propagate eastward across the Indian Ocean and Maritime Continent with sustainable amplitude. Though the latter still shows some discrepancies with the observations, the MJO is obviously well maintained in these two forecasts, confirming that if both the entrainments and detrainments of deep and shallow convections are allowed, the ECHAM4 coupled model is able to reproduce the observed MJO event during TOGA COARE with reasonable fidelity. When either deep-convection- or shallow-convection-related entrainment/detrainment is turned off, the model MJO can no longer be sustained.

Why does the forecast MJO decay quickly after turning off the entrainment/detrainment of either the shallow or deep convection? To understand the physical processes causing this sensitivity, the changes of stratiform and convective rainfall and the vertical structures of moisture in these experiments are examined. Figure 7 shows the monthly-mean rainfalls of four experiments averaged between 10°S and 10°N. In Fcst01 and Fcst02 (Table 1), the total rainfall amounts are very similar (Fig. 7a) with the intense rainfall over the Indo–western Pacific warm pool. A minimum exists around the Maritime Continent. However, the amount of the corresponding stratiform rainfall in Fcst02 is much smaller than that in the Fcst01. The averaged stratiform fraction (stratiform/total rainfall in daily mean) in the control forecast is about 40% over the Indo–western Pacific warm pool (Fcst01), which is comparable with the observations (Lin et al. 2004). On the other hand, it is only about 20% in Fcst02 (Fig. 7b)—much smaller than that in the observations and the control forecast.

The formation of stratiform rainfall in the model largely depends on the environmental relative humidity (Sundqvist 1978; Roeckner et al. 1996). The turnoff of the deep-convection-related entrainment/detrainment significantly reduces the water supply from convective plumes

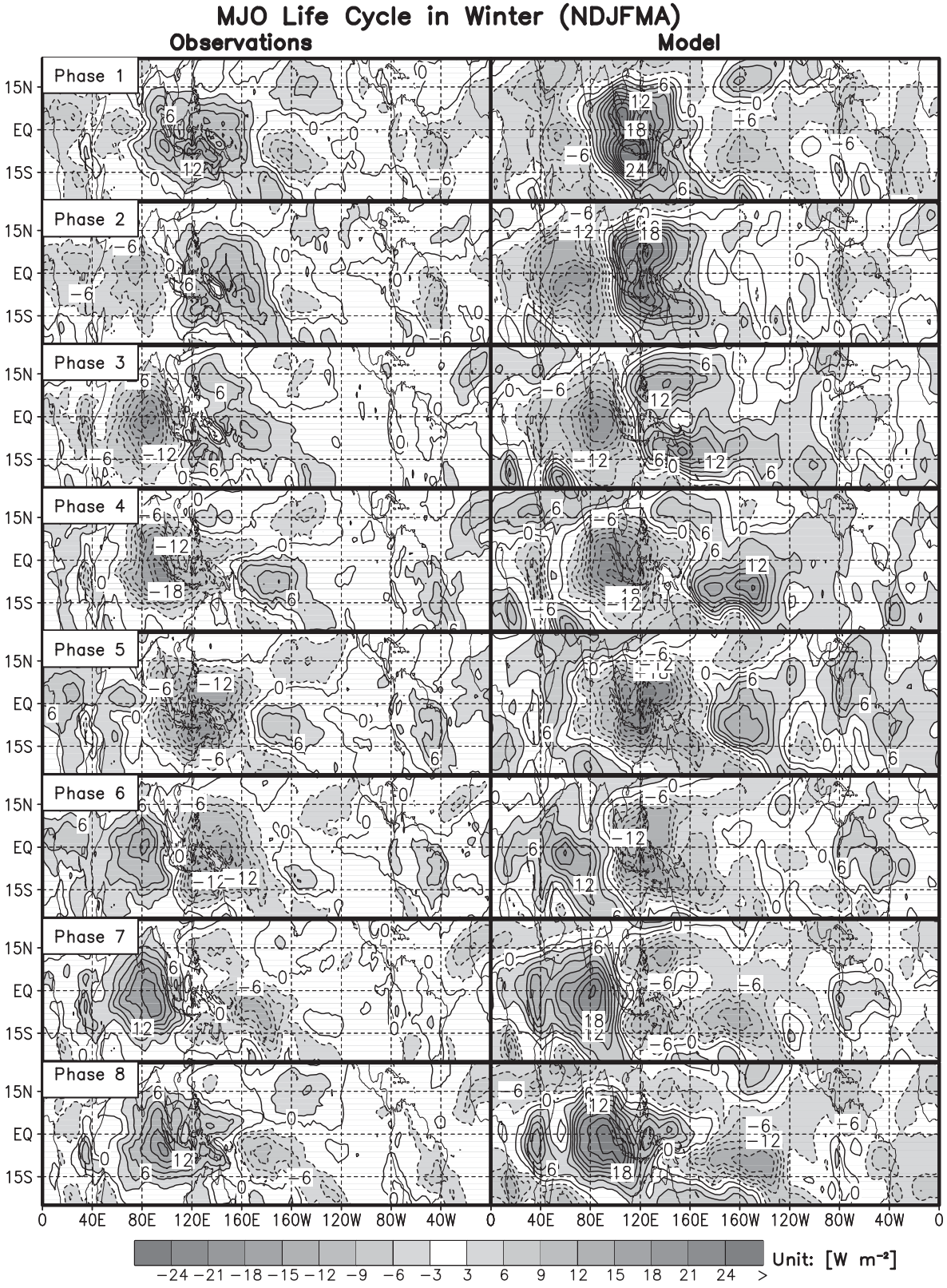

FIG. 3. The composite OLR (W m^{-2}) life cycle of the MJO for the (left) observations and (right) simulation in boreal winter (November–April).

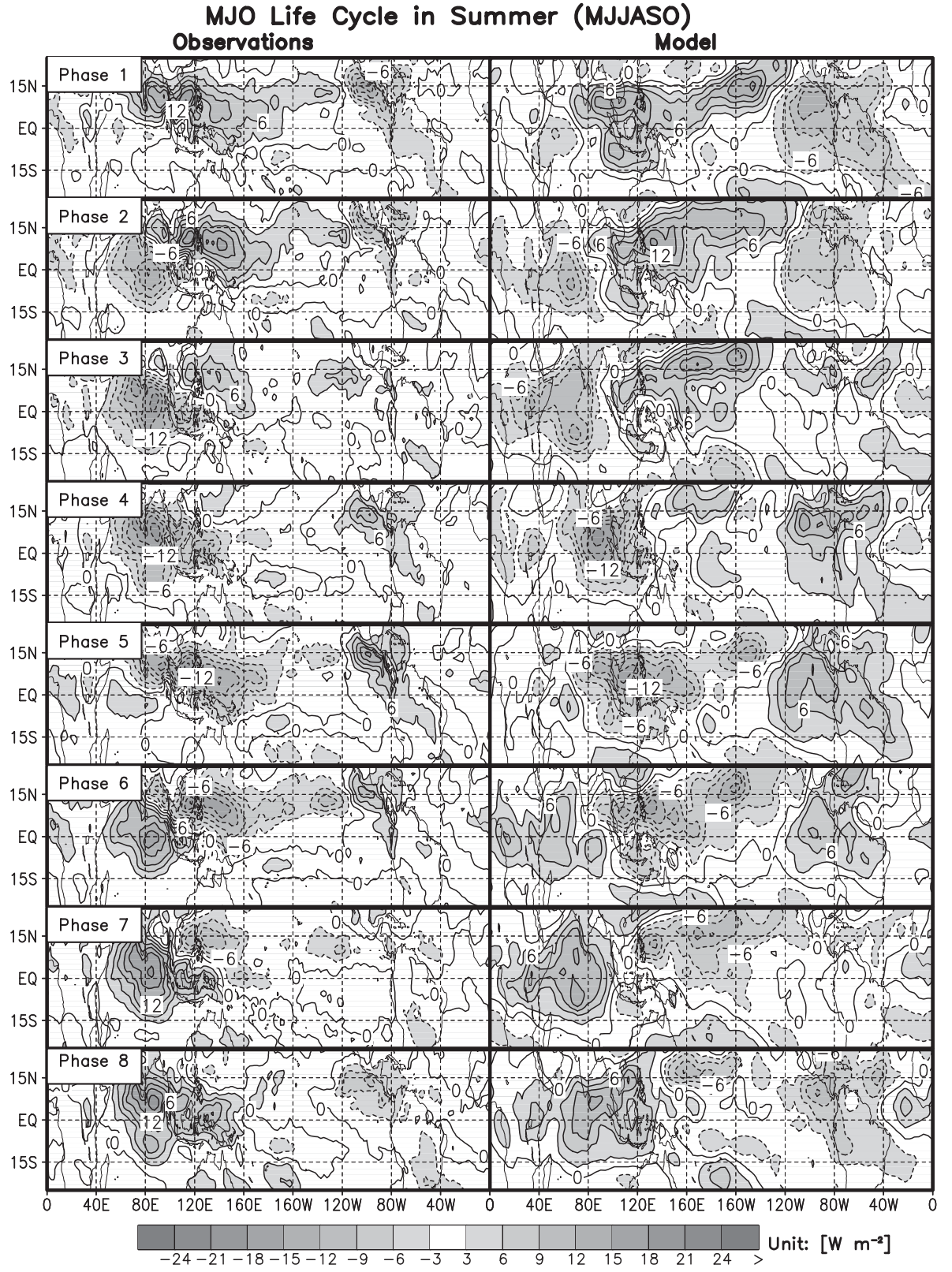

FIG. 4. The composite OLR (W m^{-2}) life cycle of the MJO for the (left) observations and (right) simulation in boreal summer [May–October (MJJASO)].

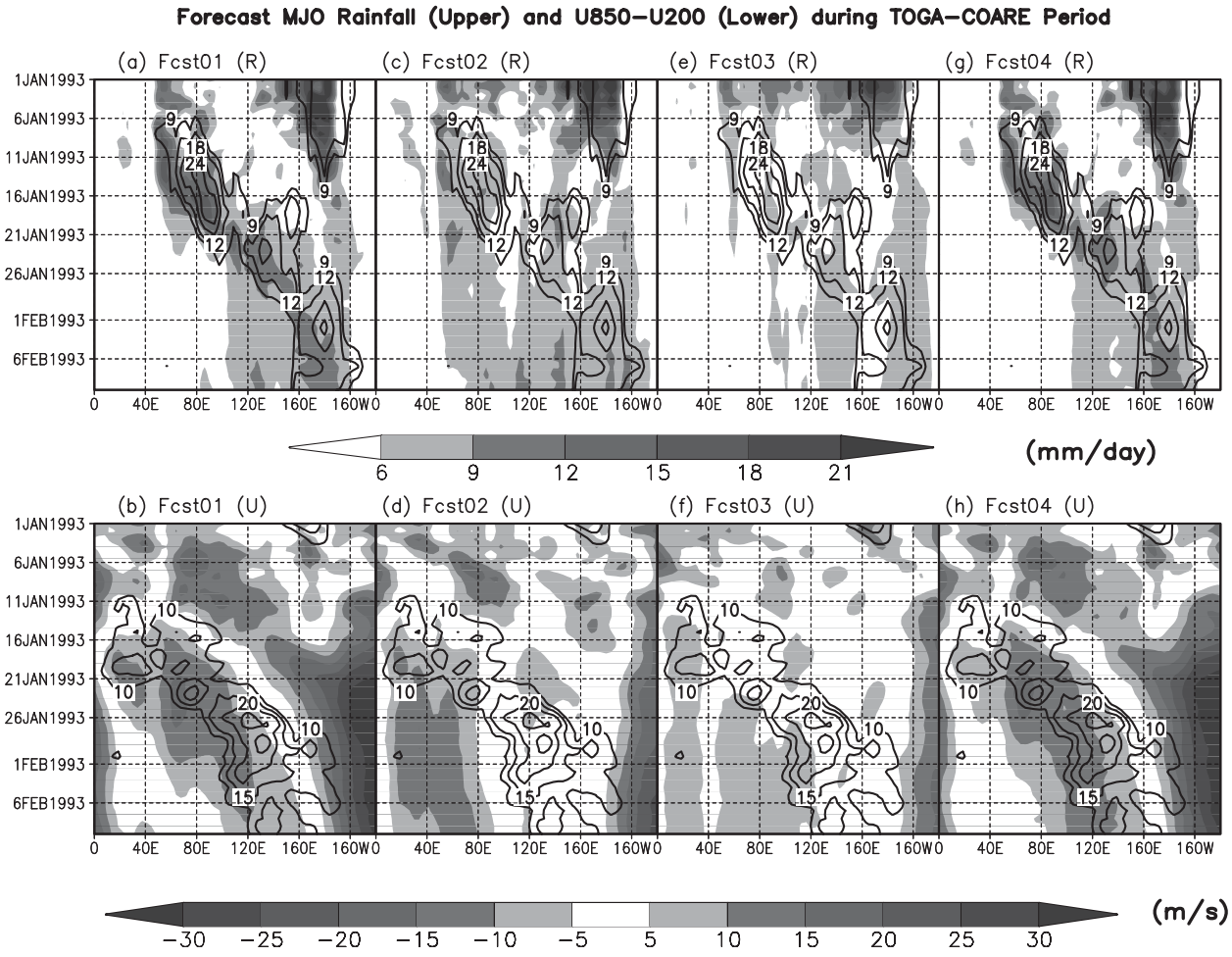

FIG. 5. (top) Rainfall (mm day^{-1}) and (bottom) vertical shear of zonal winds (m s^{-1}) from four coupled forecasts (a),(b) Fcst01; (c),(d) Fcst02; (e),(f) Fcst03; (g),(h) Fcst04. The description of the four experiments is in Table 1. The contours represent the observations; the shading shows model forecasts. All results are averaged between 10°S and 10°N.

to the environment, which results in the reduced mean relative humidity in the entire troposphere (Fig. 8a). The drier midtroposphere significantly reduces the formation of stratiform rainfall (Fig. 7b) and the associated moisture-stratiform instability (Grabowski and Moncrieff 2004; Derbyshire et al. 2004; Kuang 2008), thus resulting in the decay of model MJO. This result indicates that, even though the monthly-mean rainfall is almost the same between the two experiments, different partitions between the stratiform portion and convective portion bear important implications on the behavior of model MJO.

After turning off the entrainment/detrainment of shallow convection (Fcst03), the resultant monthly-mean rainfall shows slight decreases over the Indian Ocean and near the date line (Fig. 7c). The monthly-mean stratiform rainfall is barely seen (Fig. 7c) with an averaged fraction only about 3% (Fig. 7d), which is one order of magnitude smaller than the observations (Schumacher and Houze 2003). The consequence is that the model MJO can no longer be sustained under this condition even if it was seeded in the initial conditions (Figs. 5e and 6). As expected, the associated environmental moisture in the lower and midtroposphere was significantly reduced. Somehow, the relative humidity increases in the upper troposphere. Since the total moisture in the upper troposphere is very small (smaller than 2 g kg^{-1} above 400 hPa), this increase does not transform into significant stratiform precipitation. The results of the above two experiments (Fcst02 and Fcst03) suggest that maintaining an adequate partitioning between stratiform and convective rainfall is a critical factor to sustain the MJO in the ECHAM4 model.

b. With long-term free integration

The above forecasting experiments examined only one MJO event with a short integration (two months).

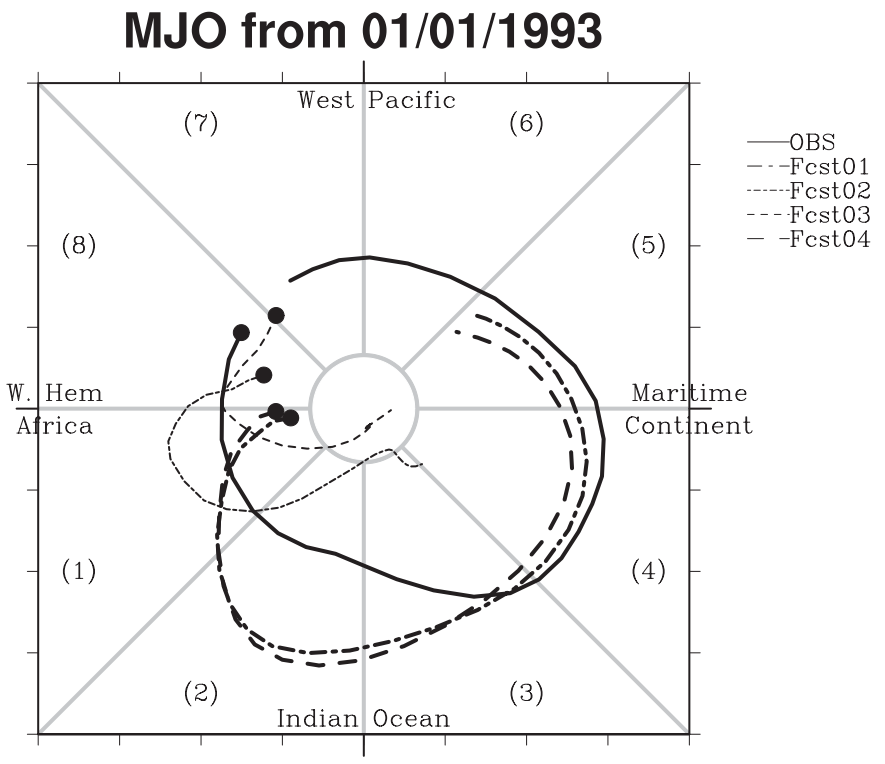

FIG. 6. Phase-space (RMM1, RMM2) trajectories of the observed (OBS) and forecast MJO from the four forecast experiments (Fcst01, Fcst02, Fcst03, and Fcst04 in Table 1).

To confirm the above findings, a suite of three 20-yr free integrations were carried out with ECHAM4 AGCM forced by climatological monthly-mean SST and sea ice.[2] In the EX01, only the entrainment/detrainment associated with deep convection is turned off. In the EX02, only the entrainment/detrainment associated with shallow convection is turned off. In the EX03, both types of entrainments/detrainments are allowed. The details of the experiments are summarized in Table 2.

Precipitation regimes are very different among the three experiments. Figure 9 shows the time–longitude rainfall evolutions averaged between 10°S and 10°N, which were derived from an individual year selected from the three experiments along with the TRMM 3B42 observations in the winter of 2002/03. After turning off the entrainment/detrainment of either the deep or shallow convection, the precipitation becomes less organized (Figs. 9a,b). No apparent eastward-propagating MJO, resembling the observations, exists. When the entrainments/detrainments of both deep and shallow convections are activated (EX03), the resultant precipitation regime (Fig. 9c) is very similar to the observations (Fig. 9d) even though the model has much coarser horizontal resolution (~3.75°) than the observations (~1°). Several MJO-like eastward-propagating rainfall systems can be easily identified from this run.

Figure 10 gives 5-yr daily precipitation time series in the equatorial western Pacific [(EQ) 160°E] from the three experiments. Though the underlying SST forcing in all three experiments is the same, the convection responses are very different. When deep-convection-related entrainment/detrainment was not allowed (EX01), the precipitation regime is dominated by high-frequency fluctuations with most daily-mean rain rate below 20 mm day^{-1}. When the shallow-convection-related entrainment/detrainment was turned off (EX02), the model produces drizzle-like rainfall in the warm-pool region with a daily-mean rain rate smaller than 10 mm day^{-1}. Since detrainments associated with the shallow and deep convections were allowed, respectively, in EX01 and EX02, the relatively stronger daily rain rate in EX01 suggests that lower-tropospheric moistening due to the shallow-convection-related detrainment may contribute more to the positive feedback between convection and circulations (Wu 2003) than that associated with deep convection alone. When the entrainments/detrainments

[2] For three long-term integrations, AGCM experiments forced with same SST and sea ice were conducted to avoid the potential complications induced by interactive air–sea coupling.

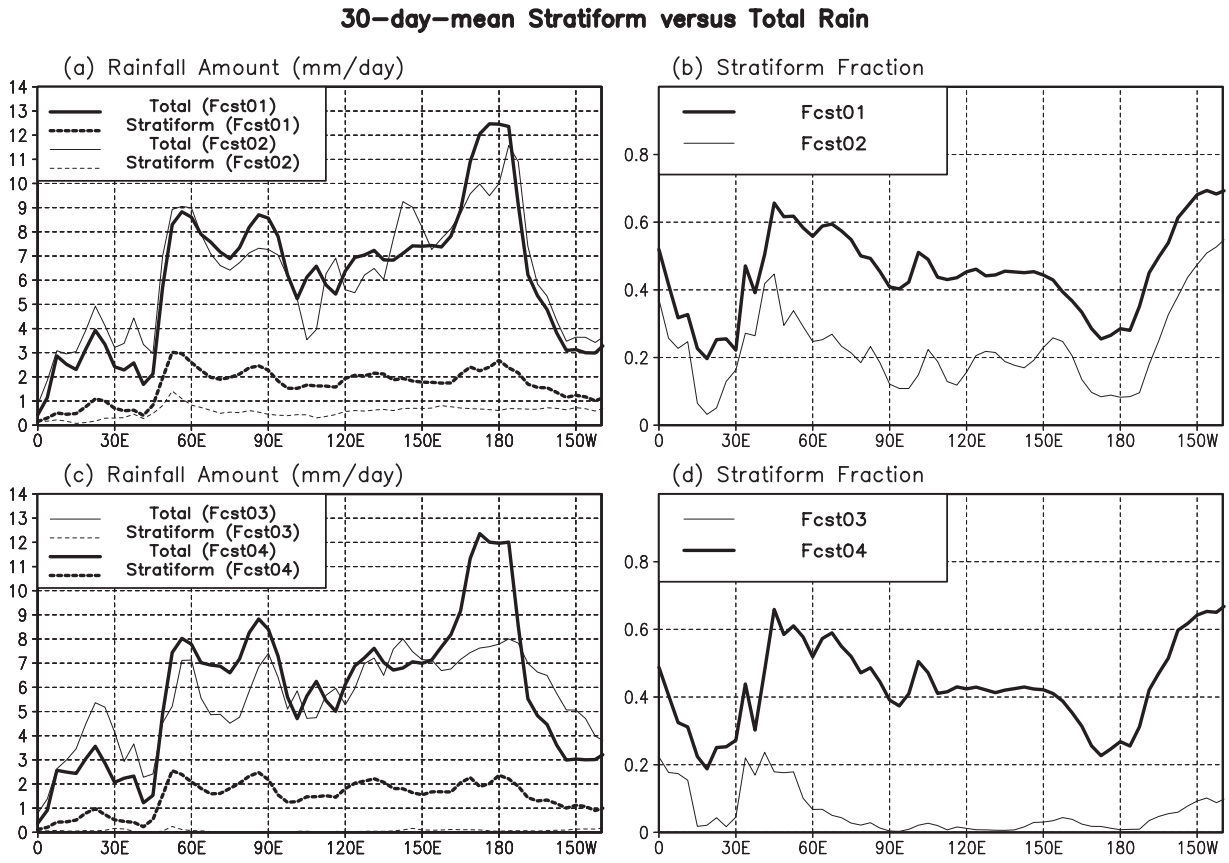

FIG. 7. Monthly-mean total rainfall, stratiform amount, and stratiform fraction (stratiform/total) for the (a),(b) Fcst01/Fcst02 and (c),(d) Fcst03/Fcst04 averaged between 10°S and 10°N.

of both deep and shallow convections were allowed (EX03), the positive feedback between convection and circulations is considerably enhanced comparing to that when only one of them was activated. The maximum daily-mean rain rate reaches 70 mm day^{-1}. These results indicate that the combined effect of the shallow- and deep-convection-related entrainments/detrainments plays an important role for the ECHAM4 model to produce extreme rainfall events.

To quantify the MJO simulated in these three long-term integrations, the last 15-yr simulations have been projected onto the observed CEOFs derived before. The resultant phase-space trajectories of three simulations have been compared to the observed one in Fig. 11. The points falling into the inner circle (with projected amplitude less than one standard deviation) represent the days having insignificant MJO signals. The circular track with sufficient amplitude represents a good equatorial eastward-propagating MJO. In the observations (Fig. 11a), many MJO events are able to maintain a proper intensity when moving around the globe. On the other hand, it is rare to see any sustained MJO-like feature in the EX01 and EX02 (Figs. 11b,c). Sometimes there are convections flaring up, but they decayed quickly. This result supports previous findings obtained under the weather forecast setting; that is, the model MJO is not sustainable when either the shallow- or deep-convection-related entrainment/detainment was excluded. When both of them are activated, the atmospheric disturbances exhibit very similar features as those observed (Fig. 11d). Many MJO-like events move around the globe with sustained amplitude. Compared to the observations, the ECHAM4 AGCM seems to lack extreme MJO events.

In addition to the equatorial eastward propagation, the MJO in boreal summer has significant northward-propagating component in the Indo–western Pacific sector (Yasunari 1979). To measure the intensity of meridionally propagating MJO in the three experiments, a limited-domain wavenumber-spectrum analysis has been conducted in a meridional direction (10°S–30°N) for boreal summer daily rainfall (Teng and Wang 2003; Fu and Wang 2004). The results of the three experiments have been summarized in Fig. 12. Similar to the eastward-propagating cases, there are no sustainable

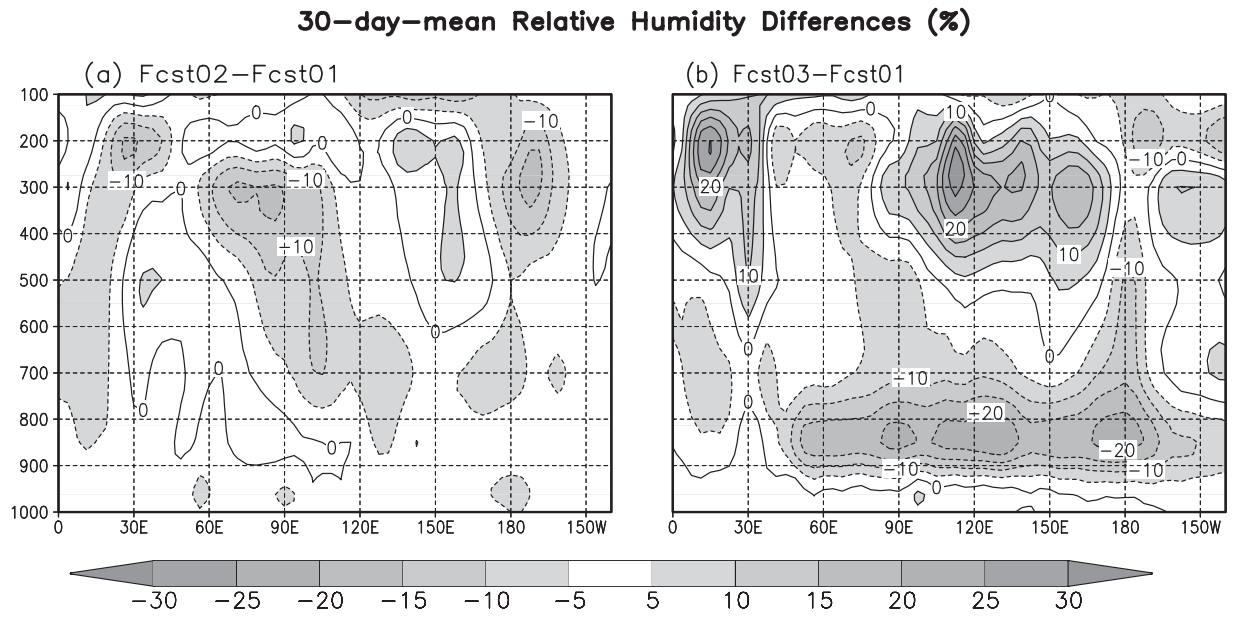

FIG. 8. Monthly-mean perturbations of relative humidity after turning off the turbulent entrainment and detrainment for the (a) deep convection and (b) shallow convection. All results are averaged between 10°S and 10°N.

meridionally propagating disturbances in either the EX01 and EX02 (Figs. 12a,b). This result indicates that, without the entrainment/detrainment associated with either the shallow or deep convection, the model is unable to sustain the large-scale convection–circulation coupling necessary for maintaining the intraseasonal disturbances no matter what the atmospheric basic state is in winter or summer. When the entrainments/detrainments associated with both the shallow and deep convection are activated, the ECHAM4 model produces significant meridionally propagating disturbances (Fig. 12c). As in the observations (Yasunari 1979), the simulated boreal summer intraseasonal disturbances show stronger northward propagation than southward propagation. However, the intensity of the simulated northward propagation is weaker than the observations

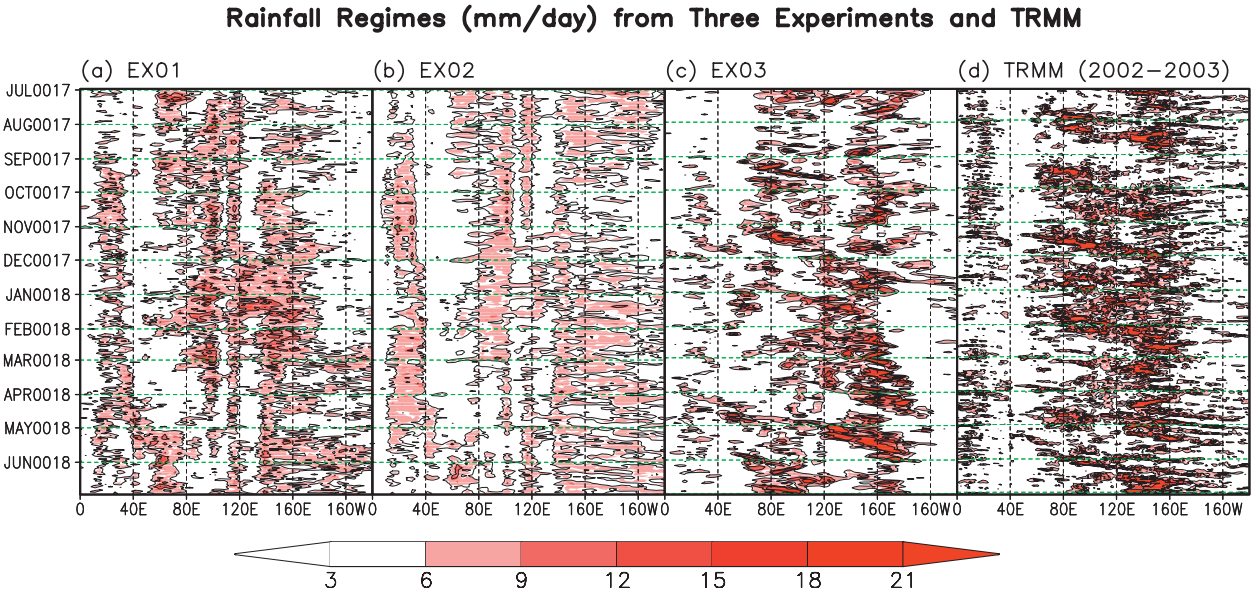

FIG. 9. One-year example of precipitation regimes averaged between 10°S and 10°N from three long-term integrations (Ex01, Ex02, and Ex03 in Table 2) along with TRMM 3B42 observations in 2002–03.

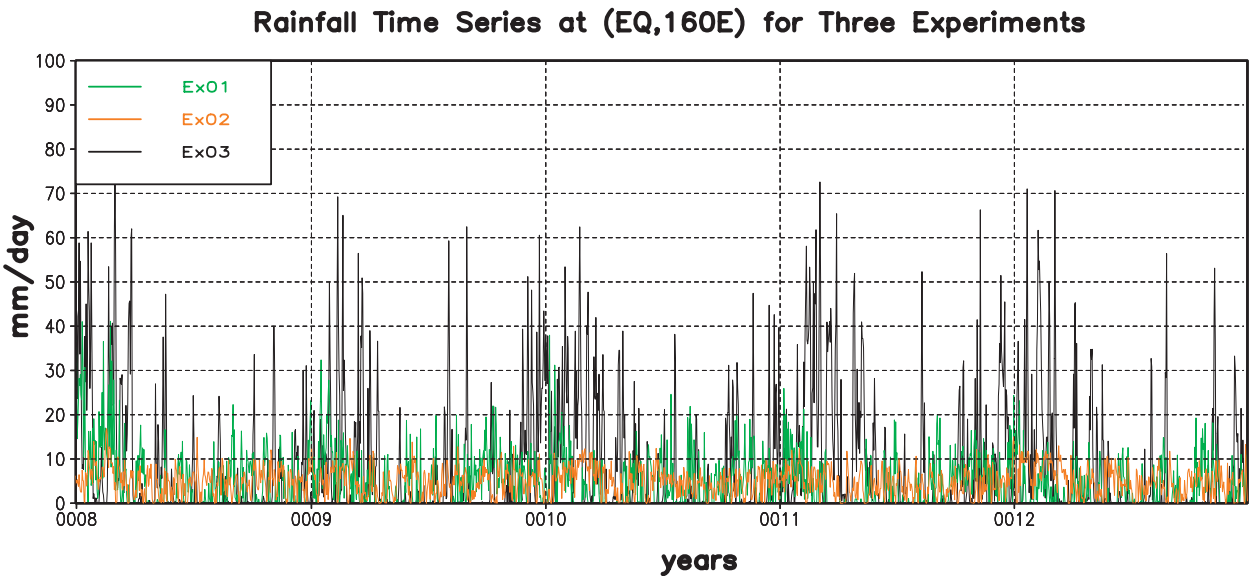

FIG. 10. Five-year precipitation time series in EQ (160°E) from three long-term integrations (Ex01, Ex02, and Ex03 in Table 2).

because of the lack of interactive air–sea coupling (Fu et al. 2003; Fu and Wang 2004).

Following the analysis under the weather forecast setting, the stratiform and total rain rates averaged in 15-yr free integrations have been given in Fig. 13. The total rain rates averaged in the Indo–western Pacific warm-pool region are similar among the three experiments, with the zonal distributions being more uniform in the EX01 and EX02 than in the EX03. A distinctive feature of the EX01 and EX02, in comparison to the EX03, is the negligibly small amount of stratiform rainfall except near the African continent and the far western Indian Ocean. The considerably small stratiform rain rates in the EX01 and EX02 are consistent with the reduced midtroposphere humidity (Fig. 14). On the other hand, the stratiform rain rate is robust in the EX03 (Fig. 13c) with an averaged fraction of about 30%, which is comparable with the observed mean value in the tropics (~40% in Schumacher and Houze 2003) but smaller than that directly associated with an MJO event (Fig. 7b). This is consistent with the result of Lin et al. (2004), who, using observational data, found that the stratiform fraction during MJO events is larger than that of climatology.

The present results from both the short-term forecasting experiments with interactive air–sea coupling and long-term free integrations under atmosphere-only context suggest that an adequate partitioning between stratiform rainfall and convective rainfall is a critical factor for contemporary general circulation models to produce a robust MJO.

5. Discussion

We have shown that, without the entrainment/detrainment associated with either the shallow or deep convection, the midtroposphere becomes abnormally dry and the amount of the stratiform rainfall in the model is significantly reduced. These changes result in the decay of the once-robust MJO in the ECHAM4 model. The dry condition in the midtroposphere is a consequence of the reduced water detrainment from the convective plumes.

But why is the stratiform rainfall considerably reduced? The reduced daily-mean rain rate (Fig. 10) after turning off the entrainment/detrainment associated with either the shallow or deep convection indicates that the upward motion and the associated moisture transports in these two cases have been significantly weakened (figure not shown). The weak convective plumes and reduced water detrained into the environment limit the water supply available for the formation of stratiform clouds, thus resulting in considerable reduction of the stratiform rainfall (Fig. 13).

Why, then, does the reduced stratiform rainfall suppress the model MJO? In the intermediate tropical atmospheric models, MJO-like disturbances can be readily simulated if a direct interaction between low-frequency equatorial waves and latent heat released in precipitation is assumed (e.g., Wang and Li 1994; Wang and Xie 1997). In the complex GCMs, the stratiform precipitation, which liberates latent heat at the grid scale, can induce a direct interaction between large-scale

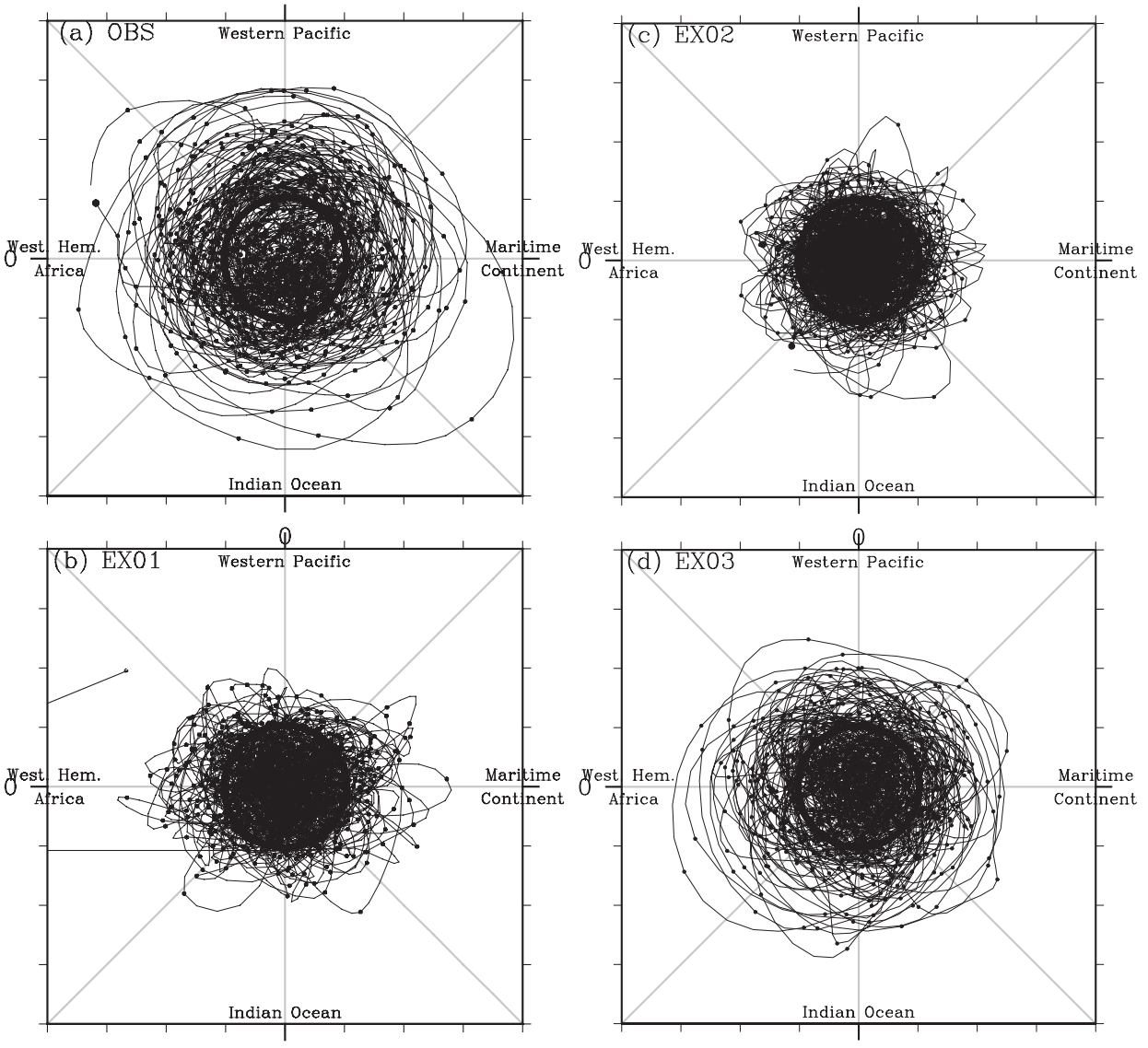

FIG. 11. Phase-space (RMM1, RMM2) trajectories of the 15-yr OLR and 850- and 200-hPa zonal winds from (a) the observations (1991–2005), (b) Ex01, (c) Ex02, and (d) Ex03 (Table 2).

waves and latent heating. Drawing upon the success of intermediate models on simulations of MJO-like low-frequency oscillations, Wang (2005) envisioned that "to simulate the MJO realistically with complex GCMs, the cumulus parameterization schemes have to allow the precipitation heating affects large-scale low-frequency waves either directly (through grid-scale precipitation for example) or indirectly (through correct description of the multiscale interactions) and to allow these low-frequency waves control the heating to some extent." The stratiform precipitation allows the direct interaction between the large-scale low-frequency waves and precipitation heating that is critical for development and maintenance of the MJO. The failure to maintain the low-frequency MJO in the EX01 and EX02 (Figs. 9, 11, and 12) may be attributed to the dominance of drizzle-like disturbances in these two cases (Fig. 10). The stratiform (or grid-scale) rainfall in the ECHAM4 model probably represents an upscale process from individual convective plumes. The enhanced stratiform rainfall in the EX03 (Fig. 13c), therefore, allows the parameterized heating to interact efficiently with the large-scale low-frequency waves and results in a sustained MJO in the model (Figs. 9c, 11d, and 12c).

Another way to argue the important role of the stratiform precipitation is to examine the vertical structures of moisture and temperature anomalies associated with MJO convection in the observations and three experiments

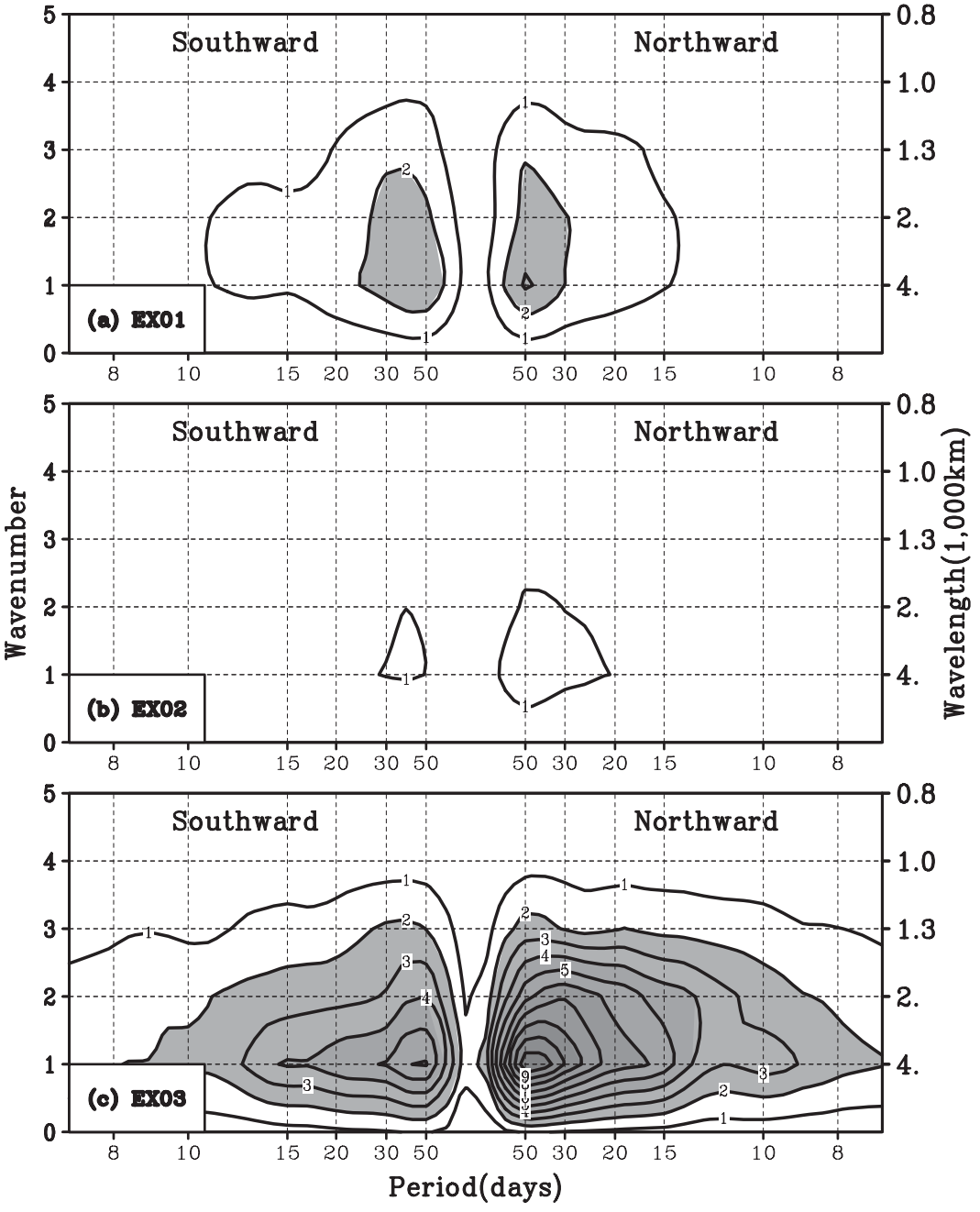

FIG. 12. Wavenumber-frequency spectra ($mm^2\ day^{-2}$) averaged between 65° and 95°E represent the northward- and southward-propagating rainfall variances in boreal summer (MJJASO) from the three experiments (a) Ex01, (b) Ex02, and (c) Ex03 (Table 2).

(EX01, EX02, and EX03). The vertical structures were derived by regressing these fields with respect to daily rainfall anomaly (Mapes et al. 2006; Kiladis and Weickmann 1992) in the equatorial western Pacific (160°E). For the model experiments, the anomalies of temperature, moisture, and rainfall are derived by removing a 15-yr daily climatology from the total fields. For the observations, four-year (2003–06) daily rainfall from TRMM 3B42 and the moisture/temperature profiles obtained by satellite *Aqua* Atmospheric Infrared Sounder (AIRS) (Chahine et al. 2006; Fu et al. 2006; Tian et al. 2006) are used.

Figure 15 shows the resultant vertical structures of moisture and temperature anomalies along with the

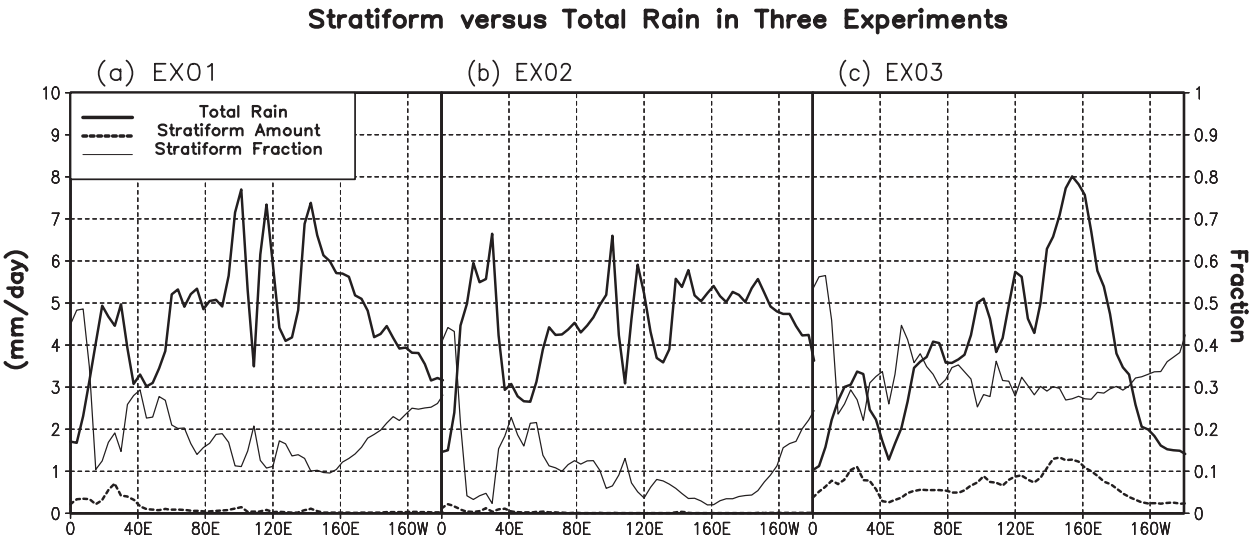

FIG. 13. Fifteen-year-mean total rainfall, stratiform amount, and stratiform fraction (stratiform/total) averaged between 10°S and 10°N for three long-term integrations (a) Ex01, (b) Ex02, and (c) Ex03.

regressed rainfall. In the observations (Fig. 15a), a lower-tropospheric moisture preconditioning appears about 10 days before the rainfall peak, as found in other studies (Sherwood 1999; Kikuchi and Takayabu 2004; Mapes et al. 2006; Yang et al. 2008; Tao et al. 2009). The follow-up deep convection moistens the entire troposphere by upward moisture transport and the water (and vapor) detrained from the convective plumes. The near-surface dry layer is probably caused by convective downdrafts (Johnson 1976; Fu et al. 2006). The vertical structure of the temperature anomaly with a positive (negative) sign in the upper (lower) troposphere signifies the important contribution of stratiform rainfall (Houze 1982; Straub and Kiladis, 2003; Lin et al. 2004).

How does the stratiform precipitation–large-scale wave interaction sustain the MJO? From energetic point of view, the covariability between the positive

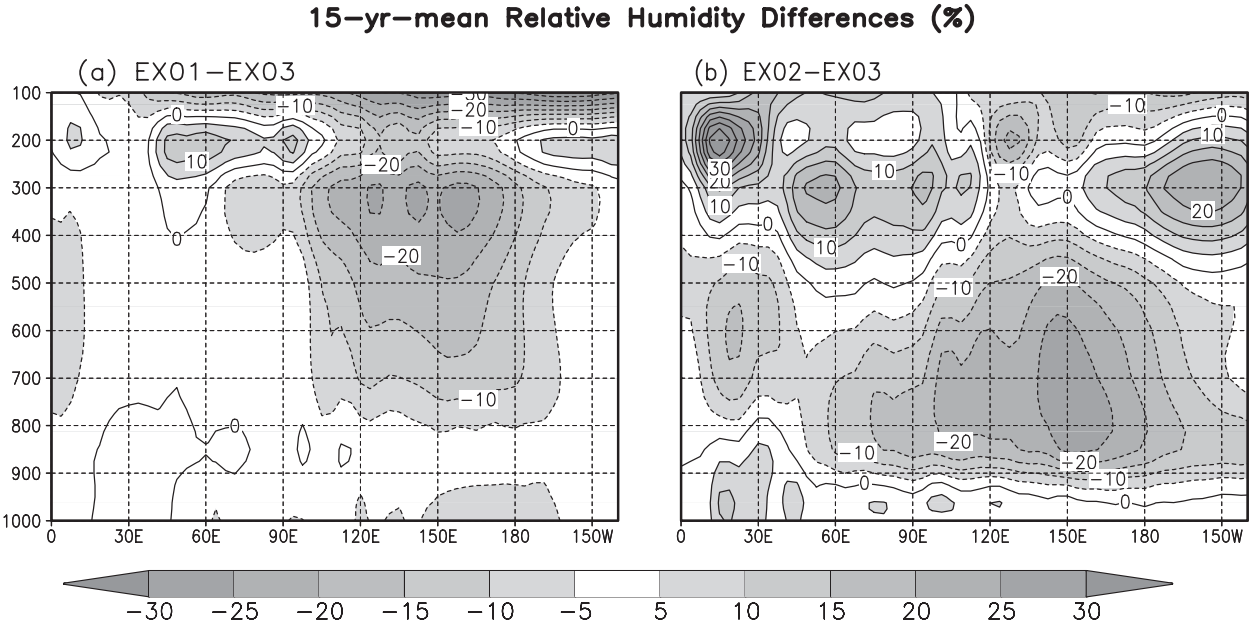

FIG. 14. Fifteen-year-mean perturbations of relative humidity after turning off the turbulent entrainment and detrainment for (a) deep convection and (b) shallow convection. All results are averaged between 10°S and 10°N.

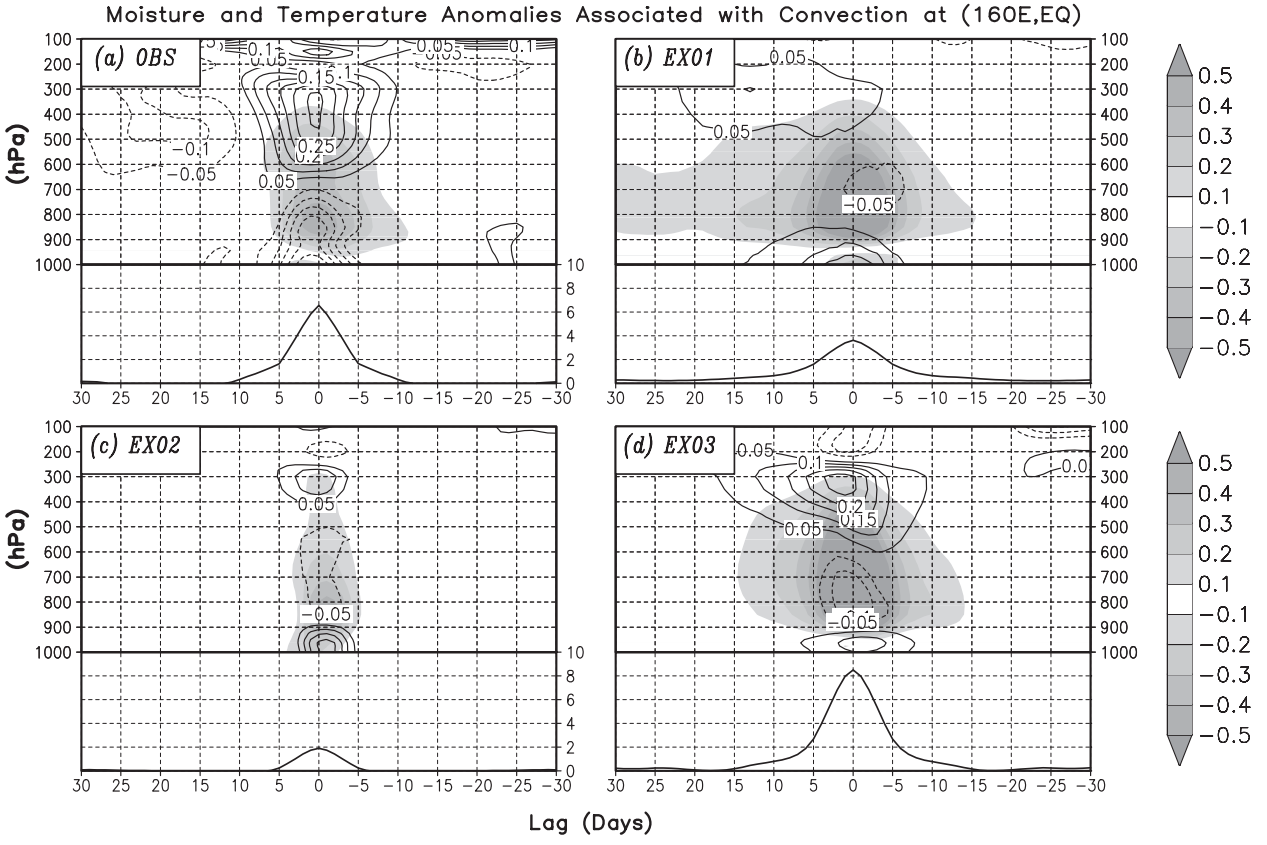

FIG. 15. Lag–height regressions of moisture (shading; g kg^{-1}) and temperature (contours; °C) perturbations overlaying on the regressed rainfall anomaly (mm day^{-1}) in EQ (160°E) for (a) the observations, (b) EX01, (c) EX02, and (d) EX03. The observed rainfall is from TRMM 3B42; the observed moisture and temperature are from satellite *Aqua* AIRS.

temperature anomaly and the heating in the upper troposphere (Fig. 15a) produces eddy available potential energy (Lau and Lau 1992) that is necessary to maintain the MJO against dissipation. This covariability is also related to the moisture-stratiform instability proposed by Mapes (2000) and Kuang (2008). Assuming that a positive temperature anomaly in the upper troposphere is initiated by convective plumes, the detrainment associated with the convection moistens the environments and favors the further development of convective plumes (Derbyshire et al. 2004) and the formation of stratiform rainfall. The latent heat released by stratiform rainfall further enhances the upper-tropospheric warming and the covariability between the positive temperature anomaly and heating, establishing a moisture-stratiform instability. By allowing the efficient interaction between the model convection and low-frequency large-scale circulations, the stratiform rainfall may also enhance other feedbacks important to the MJO in complex GCMs, for example, the frictional conditional instability of the second kind (CISK; Wang 1988), the wind-induced surface heat exchange (WISHE; Emanuel 1993), and cloud–radiation feedback (Hu and Randall 1994).

When the entrainment/detrainment associated with either the deep or shallow convection was turned off, the resultant positive (negative) temperature anomalies in the upper (lower) troposphere are considerably weaker (Figs. 15b,c) than the observations (Fig. 15a). This suggests that the contributions of the stratiform rainfall are negligible in these two cases, consistent with the results in Figs. 13a,b. The small upper-tropospheric temperature anomaly suggests the coupling between convection and large-scale circulation is too weak to sustain any MJO in the model (Figs. 11b,c). The associated tropical rainfall becomes less organized and weak (Figs. 9 and 15). This result agrees with the conjecture of Wang (2005) that the loose coupling between the parameterized heating and large-scale low-frequency waves is an important reason for the missed MJO in complex models. When both the deep- and shallow-convection-related entrainments/detrainments are allowed (EX03), the simulated vertical structures of temperature and moisture anomalies (Fig. 15d) are similar

to the observations (Fig. 15a). The apparent positive (negative) temperature anomaly in the upper (lower) troposphere (Fig. 15d) implies the significant contribution of the stratiform rainfall, which is consistent with the result of Fig. 13c. As in the observations, the significant upper-tropospheric warming and associated strong convection–circulation coupling in this case produce well-organized convection (Fig. 9c) and very large rainfall events (Fig. 15d), allowing the model to sustain a robust MJO (Figs. 11d and 12c). Although the similarity between Fig. 15a and Fig. 15d does suggest the potential importance of stratiform rainfall on the energetics of MJO, more in-depth analysis and experiments are needed to sort out the detailed physical processes through which the stratiform rainfall acts to sustain the model MJO.

6. Concluding remarks

In this study, we conducted a series of sensitivity experiments with the ECHAM4 AGCM and its coupled version (Fu et al. 2002) aiming to identify the critical processes responsible for the robust MJO in the model. Designs of the sensitivity experiments are motivated by recent observational findings that abundant stratiform rainfall (with a fraction of 40%) exists in the tropics and the MJO (Schumacher and Houze 2003; Wang et al. 2006) and the theoretical studies on the role of moisture-stratiform instability in sustaining convectively coupled equatorial waves (Mapes 2000; Straub and Kiladis 2003; Kuang 2008). Many contemporary GCMs, however, significantly underestimate the proportion of stratiform rainfall (Lin et al. 2004), which may be a caveat responsible for the weak MJO in these models. To test this hypothesis, two suites of sensitivity experiments have been carried out with the ECHAM4 model to see how the simulated MJO will change as the stratiform fraction varies: first under a weather forecast setting and then with 20-yr free integration.

Under the weather forecast setting, a series of retrospective ensemble forecasts (~60-day integrations) has been conducted to reproduce an MJO event observed during TOGA COARE. The detrainments of deep/shallow convections (as water supply for stratiform clouds) can be turned on or off, so the partition between the stratiform rainfall and convective rainfall can be changed in the model experiments. All experiments are initiated with the same NCEP reanalysis on 1 January 1993. The results indicate that only when the model produces a significant fraction (~40%) of stratiform rainfall can the forecast MJO have sustained eastward propagation across the Indian and western Pacific Oceans as in the observations.

To confirm the above finding, three more sensitivity experiments, each with a 20-yr free integration, have been conducted. When the stratiform fraction in the model is too small, precipitation regime in the tropics is dominated by continuous drizzle-like rainfall and no eastward- or northward-propagating MJO can be sustained. Only when a significant fraction of stratiform rainfall (~30%) is produced can a positive feedback between convection and large-scale circulations be sustained (Fig. 15d). This feedback plays a critical role in the development and maintenance of MJO in the ECHAM4 model.

The present results suggest that stratiform precipitation amount is a necessary condition for the ECHAM4 model to produce a robust MJO, but it may not be a sufficient condition. We do not know whether the present result is model dependent. In this regard, we urge similar sensitivity experiments to be conducted with other GCMs.[3] If the multimodel results reach similar conclusions, the representations of stratiform rainfall and its connections with the convective component in contemporary GCMs need to be seriously reconsidered to have overall success in the simulation and prediction of MJO.

Acknowledgments. This work was supported by NSF Climate Dynamics Program and NASA Earth Science Program and by the Japan Agency for Marine-Earth Science and Technology (JAMSTEC), NASA, and NOAA through their sponsorship of the IPRC. XF would like to thank Daehyun Kim for providing MJO analysis codes.

REFERENCES

Arakawa, A., and W. H. Schubert, 1974: Interaction of a cumulus cloud ensemble with the large-scale environment, Part I. *J. Atmos. Sci.,* **31,** 674–701.

Bechtold, P., M. Kohler, T. Jung, F. Doblas-Reyes, M. Leutbecher, M. J. Rodwell, F. Vitart, and G. Balsamo, 2008: Advances in simulating atmospheric variability with the ECMWF model: From synoptic to decadal time-scales. *Quart. J. Roy. Meteor. Soc.,* **134,** 1337–1351.

Bessafi, M., and M. C. Wheeler, 2006: Modulation of south Indian Ocean tropical cyclones by the Madden–Julian Oscillation and convectively coupled equatorial waves. *Mon. Wea. Rev.,* **134,** 638–656.

Boyle, J. S., and Coauthors, 2005: Diagnosis of Community Atmospheric Model 2 (CAM2) in numerical weather forecast configuration at atmospheric radiation measurement sites. *J. Geophys. Res.,* **110,** D15S15, doi:10.1029/2004JD005042.

[3] A recent sensitivity experiment of D. Kim et al. (2008, manuscript submitted to *J. Climate*; their Fig. 14) confirms that a reduced stratiform rainfall fraction in the Seoul National University (SNU) GCM significantly compromises the MJO simulation in the model.

Chahine, M. T., and Coauthors, 2006: AIRS: Improving weather forecasting and providing new data on greenhouse gases. *Bull. Amer. Meteor. Soc.,* **87,** 911–926.

Chao, W. C., and L. Deng, 1998: Tropical intraseasonal oscillation, super cloud clusters, and cumulus convection schemes. Part II: 3D aquaplanet simulations. *J. Atmos. Sci.,* **55,** 690–709.

Chen, B., and M. Yanai, 2000: Comparison of the Madden–Julian oscillation (MJO) during the TOGA COARE IOP with a 15-year climatology. *J. Geophys. Res.,* **105,** 2139–2149.

Chen, T.-C., and S.-P. Weng, 1999: Interannual and intraseasonal variations in monsoon depressions and their westward-propagating predecessors. *Mon. Wea. Rev.,* **127,** 1005–1020.

Cho, H.-R., and D. Pendlebury, 1997: Wave CISK of equatorial waves and the vertical distribution of cumulus heating. *J. Atmos. Sci.,* **54,** 2429–2440.

Derbyshire, S. H., I. Beau, P. Bechtold, J.-Y. Grandpeix, J.-M. Piriou, J.-L. Redelsperger, and P. M. M. Soares, 2004: Sensitivity of moist convection to environmental humidity. *Quart. J. Roy. Meteor. Soc.,* **130,** 3055–3079.

Ding, Q., and B. Wang, 2007: Intraseasonal teleconnection between the Eurasian wave train and Indian summer monsoon. *J. Climate,* **20,** 3751–3767.

Emanuel, K. A., 1993: The effect of convective response time on WISHE modes. *J. Atmos. Sci.,* **50,** 1763–1776.

Fu, X., and B. Wang, 2001: A coupled modeling study of the seasonal cycle of the Pacific cold tongue. Part I: Simulation and sensitivity experiments. *J. Climate,* **14,** 765–779.

——, and ——, 2004: The boreal summer intraseasonal oscillations simulated in a hybrid coupled atmosphere–ocean model. *Mon. Wea. Rev.,* **132,** 2628–2649.

——, ——, and T. Li, 2002: Impacts of air–sea coupling on the simulation of mean Asian summer monsoon in the ECHAM4 model. *Mon. Wea. Rev.,* **130,** 2889–2904.

——, ——, ——, and J. P. McCreary, 2003: Coupling between northward-propagating, intraseasonal oscillations and sea surface temperature in the Indian Ocean. *J. Atmos. Sci.,* **60,** 1733–1753.

——, ——, and L. Tao, 2006: Satellite data reveal the 3-D moisture structure of tropical intraseasonal oscillation and its coupling with underlying ocean. *Geophys. Res. Lett.,* **33,** L03705, doi:10.1029/2005GL025074.

——, ——, D. E. Waliser, and L. Tao, 2007: Impact of atmosphere–ocean coupling on the predictability of monsoon intraseasonal oscillations. *J. Atmos. Sci.,* **64,** 157–174.

——, ——, Q. Bao, P. Liu, and B. Yang, 2008a: Experimental dynamical forecast of an MJO event observed during TOGA-COARE period. *Atmos. Oceanic Sci. Lett.,* **1,** 24–28.

——, B. Yang, Q. Bao, and B. Wang, 2008b: Sea surface temperature feedback extends the predictability of tropical intraseasonal oscillation. *Mon. Wea. Rev.,* **136,** 577–597.

Gaspar, P., 1988: Modeling the seasonal cycle of the upper ocean. *J. Phys. Oceanogr.,* **18,** 161–180.

Goswami, B. N., R. S. Ajayamohan, P. K. Xavier, and D. Sengupta, 2003: Clustering of synoptic activity by Indian summer monsoon intraseasonal oscillations. *Geophys. Res. Lett.,* **30,** 1431, doi:10.1029/2002GL016734.

Grabowski, W. W., and M. W. Moncrieff, 2004: Moisture-convection feedback in the Tropics. *Quart. J. Roy. Meteor. Soc.,* **130,** 3081–3104.

Hendon, H. H., 2000: Impact of air–sea coupling on the Madden–Julian oscillation in a general circulation model. *J. Atmos. Sci.,* **57,** 3939–3952.

Houze, R. A., Jr., 1982: Cloud clusters and large-scale vertical motions in the tropics. *J. Meteor. Soc. Japan,* **60,** 396–410.

——, 1997: Stratiform precipitation in regions of convection: A meteorological paradox? *Bull. Amer. Meteor. Soc.,* **78,** 2179–2196.

Hsu, H.-H., 1996: Global view of the intraseasonal oscillation during northern winter. *J. Climate,* **9,** 2386–2406.

Hu, Q., and D. A. Randall, 1994: Low-frequency oscillations in radiative-convective systems. *J. Atmos. Sci.,* **51,** 1089–1099.

Jin, F.-F., 1996: Tropical ocean–atmosphere interaction, the Pacific cold tongue, and El Niño–Southern Oscillation. *Science,* **274,** 76–78.

——, L. L. Pan, and M. Watanabe, 2006: Dynamics of synoptic eddy and low-frequency flow interaction. Part I: A linear closure. *J. Atmos. Sci.,* **63,** 1677–1694.

Johnson, R. H., 1976: The role of convective-scale precipitation downdrafts in cumulus and synoptic-scale interactions. *J. Atmos. Sci.,* **33,** 1890–1910.

Jones, C., 2000: Occurrence of extreme precipitation events in California and relationships with the Madden–Julian oscillation. *J. Climate,* **13,** 3576–3587.

Kemball-Cook, S., B. Wang, and X. Fu, 2002: Simulation of the ISO in the ECHAM4 model: The impact of coupling with an ocean model. *J. Atmos. Sci.,* **59,** 1433–1453.

Khouider, B., and A. J. Majda, 2006: Multiscale convective parameterizations with crude vertical structure. *Theor. Comput. Fluid Dyn.,* **20,** 351–375.

Kikuchi, K., and Y. N. Takayabu, 2004: The development of organized convection associated with the MJO during TOGA COARE IOP: Trimodal characteristics. *Geophys. Res. Lett.,* **31,** L10101, doi:10.1029/2004GL019601.

Kiladis, G. N., and K. M. Weickmann, 1992: Circulation anomalies associated with tropical convection during northern winter. *Mon. Wea. Rev.,* **120,** 1900–1923.

Kim, H.-M., I.-S. Kang, B. Wang, and J.-Y. Lee, 2008: Interannual variations of the boreal summer intraseasonal variability predicted by ten atmosphere–ocean coupled models. *Climate Dyn.,* **30,** 485–496, doi:10.1007/S00382-007-0292-3.

Kuang, Z. M., 2008: A moisture-stratiform instability for convectively coupled waves. *J. Atmos. Sci.,* **65,** 834–854.

Lau, K.-H., and N.-C. Lau, 1992: The energetics and propagation dynamics of tropical summertime synoptic-scale disturbances. *Mon. Wea. Rev.,* **120,** 2523–2539.

Leary, C. A., and R. A. Houze Jr., 1980: The contribution of mesoscale motions to the mass and heat fluxes of an intense tropical convective system. *J. Atmos. Sci.,* **37,** 784–796.

Lee, M. I., I. S. Kang, and B. E. Mapes, 2003: Impacts of cumulus convection parameterization on aqua-planet AGCM simulations of tropical intraseasonal variability. *J. Meteor. Soc. Japan,* **81,** 963–992.

Liebmann, B., and D. L. Hartmann, 1984: An observational study of tropical–midlatitude interaction on intraseasonal timescales during winter. *J. Atmos. Sci.,* **41,** 3333–3350.

Lin, J.-L., B. Mapes, M. Zhang, and M. Newman, 2004: Stratiform precipitation, vertical heating profiles, and the Madden–Julian oscillation. *J. Atmos. Sci.,* **61,** 296–309.

——, and Coauthors, 2006: Tropical intraseasonal variability in 14 IPCC AR4 climate models. Part I: Convective signals. *J. Climate,* **19,** 2665–2690.

Liu, P., B. Wang, K. R. Sperber, T. Li, and G. A. Meehl, 2005: MJO in the NCAR CAM2 with the Tiedtke convective scheme. *J. Climate,* **18,** 3007–3020.

Madden, R. A., and P. R. Julian, 1972: Description of global-scale circulation cells in tropics with a 40–50 day period. *J. Atmos. Sci.,* **29,** 1109–1123.

Maloney, E. D., and D. L. Hartmann, 2000: Modulation of eastern North Pacific hurricanes by the Madden–Julian oscillation. *J. Climate,* **13,** 1451–1460.

——, and ——, 2001: The sensitivity of intraseasonal variability in the NCAR CCM3 to changes in convective parameterization. *J. Climate,* **14,** 2015–2034.

Mapes, B. E., 2000: Convective inhibition, subgrid-scale triggering energy, and stratiform instability in a toy tropical wave model. *J. Atmos. Sci.,* **57,** 1515–1535.

——, S. Tulich, J. L. Lin, and P. Zuidema, 2006: The mesoscale convection life cycle: Building block or prototype for large-scale tropical waves? *Dyn. Atmos. Oceans,* **42,** 3–29.

McCreary, J. P., and Z. J. Yu, 1992: Equatorial dynamics in a 2.5-layer model. *Prog. Oceanogr.,* **29,** 61–132.

Miura, H., M. Satoh, T. Nasuno, A. T. Noda, and K. Oouchi, 2007: A Madden–Julian Oscillation event realistically simulated by a global cloud-resolving model. *Science,* **318,** 1763–1765.

Moncrieff, M. W., M. A. Shapiro, J. M. Slingo, and F. Molteni, 2007: Collaborative research at the intersection of weather and climate. *WMO Bull.,* **56,** 204–211.

Nordeng, T. E., 1995: Extended versions of the convective parameterization scheme at ECMWF and their impact on the mean and transient activity of the model in the tropics. ECMWF Research Department Tech. Memo. 206, 41 pp.

Pan, L.-L., and T. Li, 2008: Interactions between the tropical ISO and midlatitude low-frequency flow. *Climate Dyn.,* **31,** 375–388, doi:10.1007/s00382-007-0272-7.

Phillips, T. J., and Coauthors, 2004: Evaluation parameterizations in general circulation models: Climate simulation meets weather prediction. *Bull. Amer. Meteor. Soc.,* **85,** 1903–1915.

Roeckner, E., and Coauthors, 1996: The atmospheric general circulation model ECHAM-4: Model description and simulation of present-day climate. Max Planck Institute for Meteorology Rep. 218, 90 pp.

Schumacher, C., and R. A. Houze Jr., 2003: Stratiform rain in the tropics as seen by the TRMM precipitation radar. *J. Climate,* **16,** 1739–1756.

Sherwood, S. C., 1999: Convective precursors and predictability in the tropical western Pacific. *Mon. Wea. Rev.,* **127,** 2977–2991.

Slingo, J. M., and Coauthors, 1996: Intraseasonal oscillations in 15 atmospheric general circulation models: Results from am AMIP diagnostic subproject. *Climate Dyn.,* **12,** 325–357.

Sperber, K. R., and H. Annamalai, 2008: Coupled model simulations of boreal summer intraseasonal (30–50 day) variability, Part 1: Systematic errors and caution on use of metrics. *Climate Dyn.,* **31,** 345–372, doi:10.1007/s00382-008-0367-9.

——, S. Gualdi, S. Legutke, and V. Gayler, 2005: The Madden–Julian Oscillation in ECHAM4 coupled and uncoupled general circulation models. *Climate Dyn.,* **25,** 117–140.

Straub, K. H., and G. N. Kiladis, 2003: The observed structure of convectively coupled Kelvin waves: Comparison with simple models of coupled wave instability. *J. Atmos. Sci.,* **60,** 1655–1668.

Sundqvist, H., 1978: A parameterization scheme for non-convective condensation including prediction of cloud water content. *Quart. J. Roy. Meteor. Soc.,* **104,** 677–690.

——, E. Berge, and J. E. Kristjansson, 1989: Condensation and cloud parameterization studies with a mesoscale numerical weather prediction model. *Mon. Wea. Rev.,* **117,** 1641–1657.

Tao, L., X. Fu, and W. S. Lu, 2009: Moisture structure of the quasi-biweekly mode revealed by AIRS in western Pacific. *Adv. Atmos. Sci.,* **26,** 513–522.

Teng, H., and B. Wang, 2003: Interannual variations of the boreal summer intraseasonal oscillation in the Asian–Pacific region. *J. Climate,* **16,** 3572–3584.

Tian, B. J., D. E. Waliser, E. J. Fetzer, B. H. Lambrigtsen, Y. L. Yung, and B. Wang, 2006: Vertical moist thermodynamic structure and spatial–temporal evolution and the MJO in AIRS observations. *J. Atmos. Sci.,* **63,** 2462–2484.

Tiedtke, M., 1989: A comprehensive mass flux scheme for cumulus parameterization in large-scale models. *Mon. Wea. Rev.,* **117,** 1779–1800.

Tokioka, T., K. Yamazaki, A. Kitoh, and T. Ose, 1988: The equatorial 30–60 day oscillation and the Arakawa-Schubert penetrative cumulus parameterization. *J. Meteor. Soc. Japan,* **66,** 883–901.

Toth, Z., M. Pena, and A. Vintzileos, 2007: Bridging the gap between weather and climate forecasting: Research priorities for intraseasonal prediction. *Bull. Amer. Meteor. Soc.,* **88,** 1427–1429.

Waliser, D. E., 2005: Predictability of tropical intraseasonal variability. *The Predictability of Weather and Climate,* T. Palmer and R. Hagedorn, Eds., Cambridge University Press, 275–305.

——, K. M. Lau, and J. H. Kim, 1999: The influence of coupled sea surface temperatures on the Madden–Julian oscillation: A model perturbation experiment. *J. Atmos. Sci.,* **56,** 333–358.

——, and Coauthors, 2003a: AGCM simulations of intraseasonal variability associated with the Asian summer monsoon. *Climate Dyn.,* **21,** 423–446.

——, K. M. Lau, W. Stern, and C. Jones, 2003b: Potential predictability of the Madden–Julian oscillation. *Bull. Amer. Meteor. Soc.,* **84,** 33–50.

——, and Coauthors, 2009: MJO simulation diagnostics. *J. Climate,* **22,** 3006–3030.

Wang, B., 1988: Dynamics of tropical low-frequency waves: An analysis of the moist Kelvin wave. *J. Atmos. Sci.,* **45,** 2051–2065.

——, 2005: Theory. *Tropical Intraseasonal Oscillation in the Atmosphere and Ocean,* W. K.-M. Lau and D. E. Waliser, Eds., Praxis Publishing, 307–351.

——, and T. Li, 1994: Convective interaction with boundary-layer dynamics in the development of a tropical intraseasonal system. *J. Atmos. Sci.,* **51,** 1386–1400.

——, and X. Xie, 1997: A model for the boreal summer intraseasonal oscillation. *J. Atmos. Sci.,* **54,** 72–86.

——, T. Li, and P. Chang, 1995: An intermediate model of the tropical Pacific Ocean. *J. Phys. Oceanogr.,* **25,** 1599–1616.

——, P. Webster, K. Kikuchi, T. Yasunari, and Y. Qi, 2006: Boreal summer quasi-monthly oscillation in the global tropics. *Climate Dyn.,* **27,** 661–675.

Wang, W., and M. E. Schlesinger, 1999: The dependence on convection parameterization of the tropical intraseasonal oscillation simulated by the UIUC 11-layer atmospheric GCM. *J. Climate,* **12,** 1423–1457.

Weickmann, K. M., G. R. Lussky, and J. E. Kutzbach, 1985: Intraseasonal (30–60 day) fluctuations of outgoing longwave radiation and 250-mb streamfunction during northern winter. *Mon. Wea. Rev.,* **113,** 941–961.

Wheeler, M. C., and H. H. Hendon, 2004: An all-season real-time multivariate MJO index: Development of an index for monitoring and prediction. *Mon. Wea. Rev.,* **132,** 1917–1932.

Wu, Z. H., 2003: A shallow CISK, deep equilibrium mechanism for the interaction between large-scale convection and large-scale circulations in the tropics. *J. Atmos. Sci.,* **60,** 377–392.

Xie, S. C., M. Zhang, J. S. Boyle, R. T. Cederwall, G. L. Potter, and W. Lin, 2004: Impact of a revised convective triggering mechanism on Community Atmosphere Model, Version 2, simulations: Results from short-range weather forecasts. *J. Geophys. Res.,* **109,** D14102, doi:10.1029/2004JD004692.

Yang, B., X. Fu, and B. Wang, 2008: Atmosphere–ocean conditions jointly guide convection of the Boreal Summer Intraseasonal Oscillation: Satellite observations. *J. Geophys. Res.,* **113,** D11105, doi:10.1029/2007JD009276.

Yasunari, T., 1979: Cloudiness fluctuations associated with the Northern Hemisphere summer monsoon. *J. Meteor. Soc. Japan,* **57,** 227–242.

Zhang, C., M. Dong, S. Gualdi, H. H. Hendon, E. D. Maloney, A. Marshall, K. R. Sperber, and W. Wang, 2006: Simulations of the Madden–Julian Oscillation in four pairs of coupled and uncoupled global models. *Climate Dyn.,* **27,** 573–592, doi:10.1007/S00382-006-0148-2.